

Title: Comprehensive molecular characterization of multifocal glioblastoma proves their monoclonal origin and reveals novel insights into clonal evolution and heterogeneity of glioblastomas

Journal: *Neuro-Oncology*

Authors: Khalil Abou-El-Ardat, Michael Seifert, Kerstin Becker, Sophie Eisenreich, Matthias Lehmann, Karl Hackmann, Andreas Rump, Gerrit Meijer, Beatriz Carvalho, Achim Temme, Gabriele Schackert, Evelin Schröck, Dietmar Krex, Barbara Klink

Contact author address: Institute for Clinical Genetics, Faculty of Medicine Carl Gustav Carus, TU Dresden, Fetscherstrasse 74, 01307 Dresden, Germany, E-mail: barbara.klink@tu-dresden.de

Patient	Gender	Age in years	Tumor localization	Focus
1	F	68	left frontal lobe	Focus 1
			right temporal lobe	Focus 2
2	M	60	right high frontal lobe	Focus 1
			right nucleus caudatus	Focus 2
3	M	74	left parietal lobe	Focus 1
			left frontal lobe	Focus 2
4	M	74	right frontal lobe	Focus 1
			right parieto-occipital lobe	Focus 2
5*	M	56	right gyrus precentralis	Focus 1
			right frontal gyrus medius	Focus 2
			right frontal gyrus superior	Focus 3
6	M	72	right frontal lobe	Focus 1
			left frontal lobe	n. a.

Table 1 Clinical Data of multifocal GBM patients Age at diagnosis. Abbreviations: F = female, M = male, n. a. = not available. *Patient from Krex et al. 2003 [1].

Gene	Region	Primer (F)	Primer (R)
<i>TP53</i>	Exon 1	CCATTTCTTTGCTTCCTC	CAGAGAGGACTCATCAAGTTCAG
<i>TP53</i>	Exon 2	GGGTTGGAAGTGTCTCATGC	TCCCACAGGTCTCTGCTAGG
<i>TP53</i>	Exon 3	AGCGAAAATTCCATGGGACTG	TCATCTGGACCTGGGTCTTC
<i>TP53</i>	Exon 4	TGGATGATTTGATGCTGTCC	GGCATTGAAGTCTCATGGAA G
<i>TP53</i>	Exon 5	CACTTGTGCCCTGACTTTCA	TGTGGAATCAACCCACAGC
<i>TP53</i>	Exon 5	CAACAAGATGTTTTGCCAACTG	AACCAGCCCTGTCGTCTCT
<i>TP53</i>	Exon 6	AGAGACGACAGGGCTGGTT	ACCACCCTTAACCCCTCCTC
<i>TP53</i>	Exon 7	TGCTTGCCACAGGTCTCC	GTCAGCGGCAAGCAGAG
<i>TP53</i>	Exon 8	GGGACAGGTAGGACCTGATTT	TAACTGCACCCTTGGTCTCC
<i>TP53</i>	Exon 9	TGCAGTTATGCCTCAGATTCA	AGAAAACGGCATTGAGTG
<i>TP53</i>	Exon 10	TGCATGTTGCTTTTGTACCG	GAAGGCAGGATGAGAATGGA
<i>TP53</i>	Exon 11	TGTCATCTCTCCTCCCTGCT	AAATGGAAGTCTGGGTGCT
<i>TP53</i>	Exon 11	CTGGAAGGGTCAACATCTTTT	AGTAGCCTGCACTGGCGTTC
<i>IDH1</i>	Exon 4	ACCAAATGGCACCATACGA	TTCATACCTTGCTTAATGGGT GT
<i>IDH2</i>	Exon 4	GCTGCAGTGGGACCACTATT	TGTGGCCTTGTACTGCAGAG
<i>PTEN</i>	Exon 1	ATCAGCTACCGCCAAGTCC	CCAGGCAAGAGTTCGGTCTA
<i>PTEN</i>	Exon 2	TATTACTCCAGCTATAGTGGGG	AGGTACGGTAAGCCAAAAA TG
<i>PTEN</i>	Exon 3	CACTTAAATGGTATTTGAGATTAG	CTCACTCTAACAAGCAGATAA C
<i>PTEN</i>	Exon 4	CAGGCAATGTTTGTAGTATTAG	GGATGACTCATTATTGTTATG AC
<i>PTEN</i>	Exon 5	GTATGCAACATTTCTAAAGTTAC	TCAATTACACCTCAATAAAAC
<i>PTEN</i>	Exon 6	CCAGTTACCATAGCAATTTAGT	GTAAACTTCTAGATATGGTTA AG
<i>PTEN</i>	Exon 7	TAAAATCGTTTTTGACAGTTTGAC	GAAAACAAATTATAGTTCCTT ACA
<i>PTEN</i>	Exon 8	ACTTTTTGCAAATGTTTAACATAG	TCATGTTACTGCTACGTAAAC AC
<i>PTEN</i>	Exon 9	GGCCTCTTAAAGATCATGTTTG	GGTCCATTTTCAGTTTATTCA AG
<i>EGFR</i>	Exon 1(F) 1&8(R)	GAGCTCTTCGGGGAGCAG	GTGATCTGTCACCACATAATT ACCTTTCT
<i>EGFR</i>	Exon 1(F) Exon 8(R)	GAGCTCTTCGGGGAGCAG	TCCTCCATCTCATAGCTGTCC
<i>TERT</i>	Promoter	GGCCGATTGACCTCTCT	AGCACCTCGCGGTAGTGG

Table 2: Primer sequences used in this study. F=forward, R=reverse

Probe ID	Patient	Focus	Fold-change
A_23_P2181;A_33_P3381265	Patient 1	1	-0.707690489027701
A_23_P2181;A_33_P3381265	Patient 1	2	-2.14235609321007
A_23_P2181;A_33_P3381265	Patient 2	1	-1.54756377151333
A_23_P2181;A_33_P3381265	Patient 2	2	-3.09378884701493
A_23_P2181;A_33_P3381265	Patient 4	1	-2.80493748084829
A_23_P2181;A_33_P3381265	Patient 6	1	-0.594910935618801

Table 3: Expression of CYB5R2 (ENSG00000166394) in six foci from four patients with multifocal GBM compared to three commercially available RNA of normal human brain samples. The probe IDs are from the Agilent 8x60K DNA microarray chips.

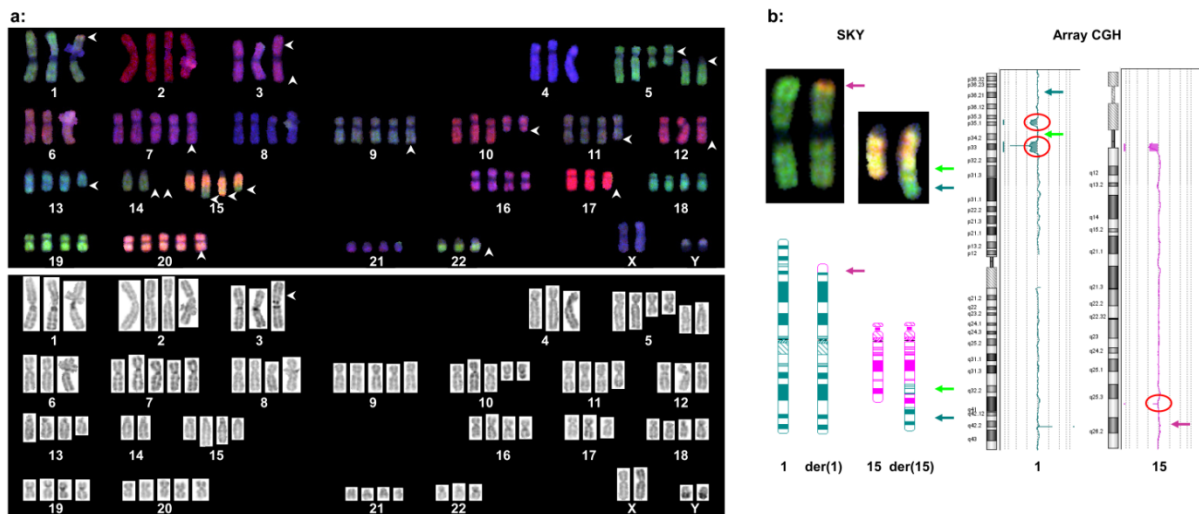


Figure S1 Numerical and structural chromosome aberrations in tumor focus 3 of patient 5

a: A representative SKY karyogram is given for a primary tumor cell line derived from tumor focus 3 of patient 5. Chromosomes are arranged in numerical order and each chromosome is shown in the SKY display (above) and after staining with DAPI (below). SKY analysis revealed multiple numerical and structural chromosomal aberrations (arrowheads) as well as a hypotetraploid karyotype:

60~90,XXYY,-1,der(1)t(1;15)(p3?3;q2?6.1),-3,idic(3)(p11.2),-4,der(5)del(5)(p12)del(5)(q?11.2q?13)x2,+i(5)(p10)x2,+7,+9,+10,del(10)(q2?1.2)x2,del(11)(q2?3),-12,del(13)(q?14q?31),-14,-14,der(15)t(1;15)(p3?4.3;q2?6.1)ins(15;1)(q2?4;p3?4.3p3?3)x2[11],der(15)ins(15;1)(q2?4;p3?4.3p3?3)t(15;15)(q2?5;q2?5)[11],der(15)t(1;15)(p3?4.3;q25)[11],-17,+20,-22[cp22].

Eleven of 22 analyzed metaphase spreads showed two derivative chromosomes 15 [der(15)t(1;15)(p3?4.3;q2?6.1)ins(15;1)(q2?4;p3?4.3p3?3)] and two normal chromosomes 15, which was also seen in focus 1 and 3 from patient 5. The other 11/22 analyzed cells from tumor focus 3 of patient 5 showed one normal chromosome 15, one derivative 15 der(15)t(1;15)(p3?4.3;q2?6.1)ins(15;1)(q2?4;p3?4.3p3?3) and two additional derivative 15 due to an additional rearrangement between the remaining normal and derivative chromosomes 15 resulting in der(15)ins(15;1)(q2?4;p3?4.3p3?3)t(15;15)(q2?5;q2?5) and der(15)t(1;15)(p3?4.3;q25), as shown in this figure.

b: The complex chromosomal rearrangement between chromosomes 1 and 15 led to derivative chromosomes der(1) [der(1)t(1;15)(p3?3;q2?6.1)] and der(15) [der(15)t(1;15)(p3?4.3;q2?6.1)ins(15;1)(q2?4;p3?4.3p3?3)] seen in SKY and resulted in two small deletions on chromosome 1 (app. 3.6 Mb deletion on 1p35.1p34.3 and app. 6.9 Mb deletion on 1p33p32.3) and one small deletion on chromosome 15 (app. 200 kb deletion on 15q26.1) seen in array CGH. The identical rearrangement and identical deletions were present in all three tumor foci from patient 5 (see Table 3). Upper left: SKY display of representative chromosomes 1 and 15 and derivative chromosomes der(1) and der(15). Lower left: Chromosome ideograms using Cytogenetic Data Analysis System (CyDAS, www.cydias.org). Right: Representative array CGH result for chromosomes 1 and 15. Arrows indicate the rearranged chromosome material identified using SKY. Red circles indicate the lost (deleted) chromosome material seen in array CGH. der = derivative chromosome

EGFRvIII is present in focus 1 but not in focus 2 of patient 3

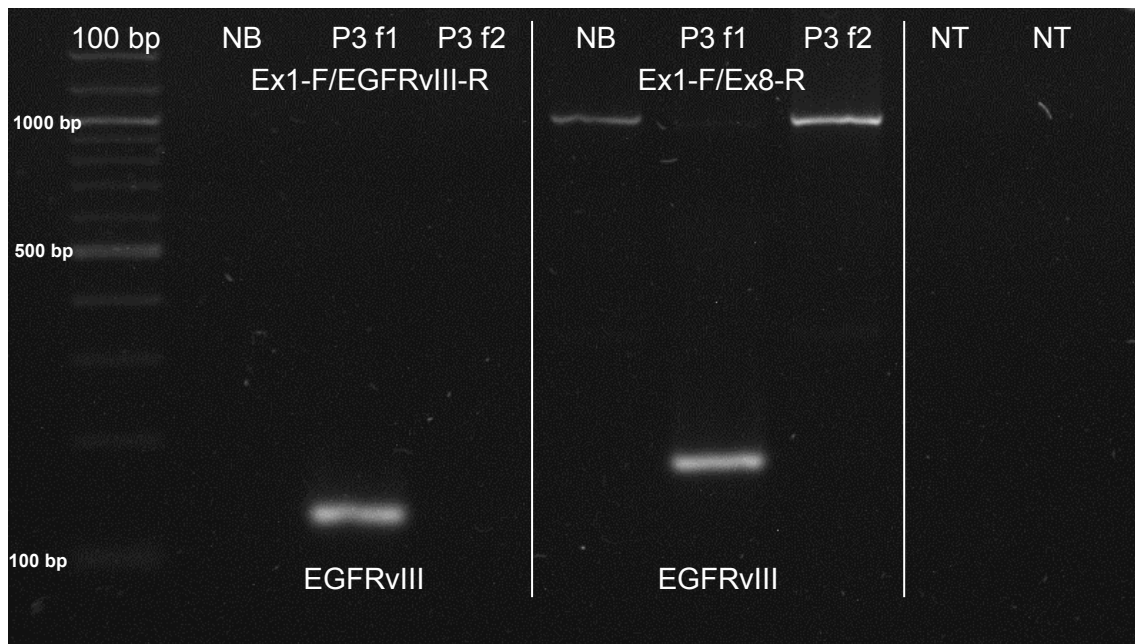


Figure S2: reverse transcriptase polymerase chain reaction (RT-PCR) proves the presence of EGFRvIII (EGFR. Δ 2-7) in tumor focus 1 from patient 3 (P3 f1) but wild-type EGFR in focus 2 from the same patient (P3 f2).

We used the primer pair published by Yoshimoto *et al.* (EGFRvIII-1) which we here call Ex1-F/EGFRvIII-R spanning the deletion [2]. The reverse primer is designed as to bind on the cDNA sequence created by the fusion of exons 1 and 8 of *EGFR* and therefore will only give a product when exons 2 through 7 are deleted. This primer pair is thus specific for the EGFRvIII variant and should give no product with wild-type *EGFR*. We also used a primer pair on exons 1 and 8 (herewith denoted by Ex1-F/Ex8-R) that would give a 979-bp product with wild-type *EGFR* and a 132-bp product with *EGFRvIII*. Using the primer pair Ex1-F/EGFRvIII-R, we only got a product of around 131-bp with cDNA from focus 1 from patient 3 (P3 f1; lane 3) but not from normal brain sample (NB; lane 2) or cDNA from focus 2 from the same patient (P3 f2; lane 4) indicating the presence of *EGFRvIII* in this tumor only. When the other primer pair was used (Ex1-F/Ex8-R), a single 979-bp product was obtained from the cDNA of normal brain (NB; lane 5) and that from focus 2 from patient 3 (P3 f2; lane 7); however, two products were obtained from the cDNA of focus 1 from patient 3 (P3f1; lane 6): a faint band at 979-bp and a stronger band at 132 bp indicating the presence of both *EGFRvIII* (132-bp product) and wild-type *EGFR* (979 product) in focus 1 from patient 3 but only wt *EGFR* in the other focus from the same patient. Lane 1 contained a 100-bp molecular weight ladder. NB = normal brain (Clontech Human Fetal Brain Total RNA), NT = non-template control for Ex1-F/EGFRvIII-R and Ex1-F/Ex8-R respectively.

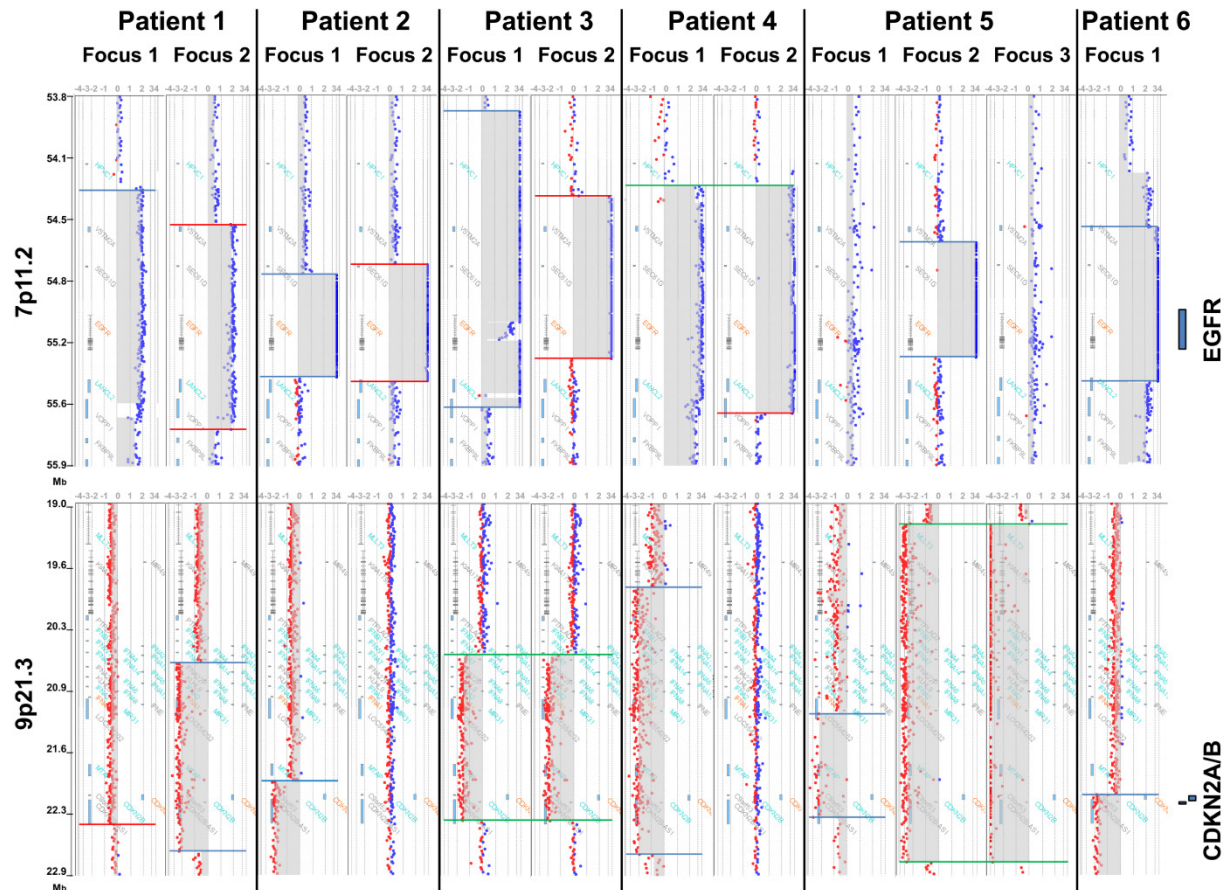
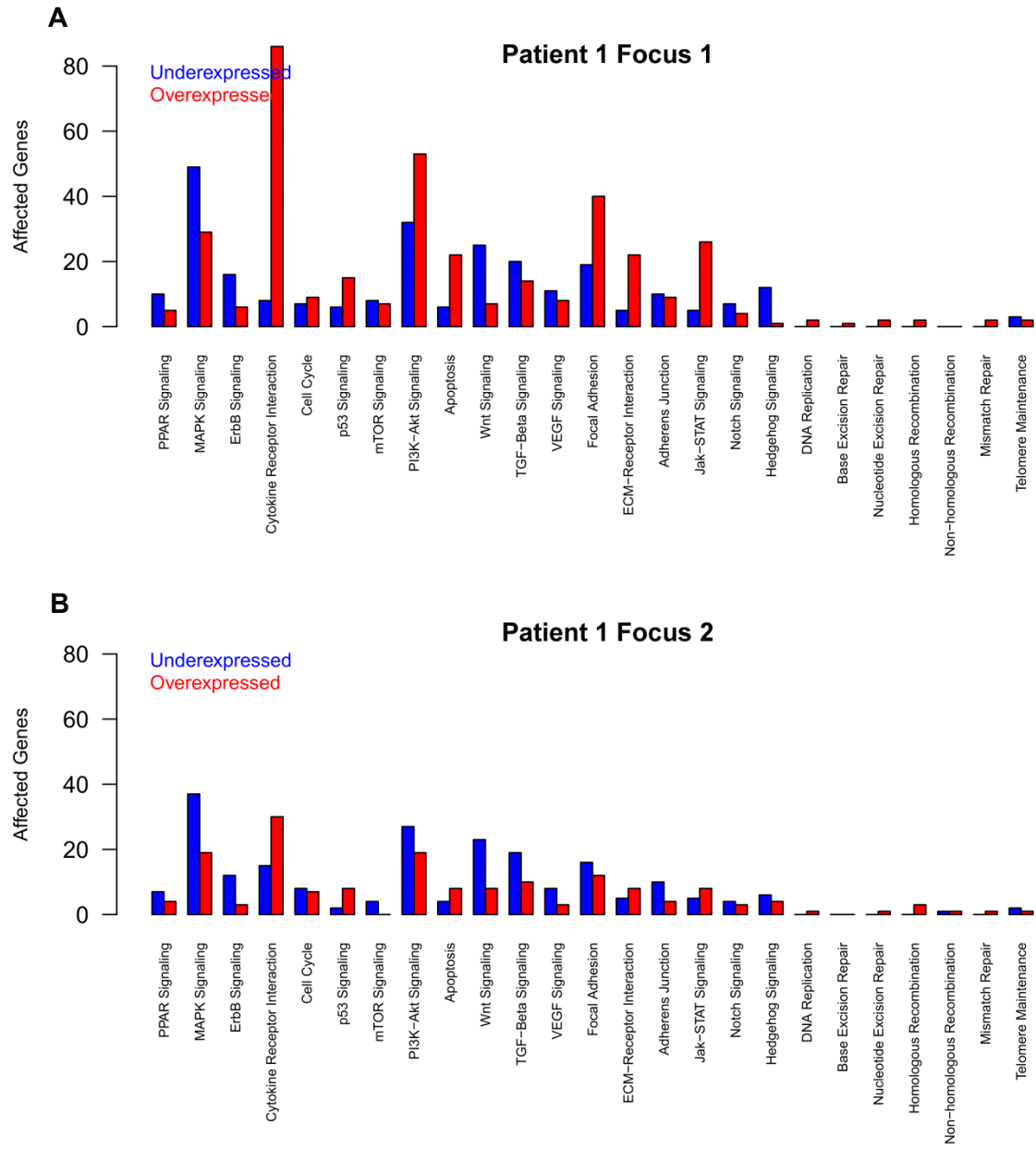
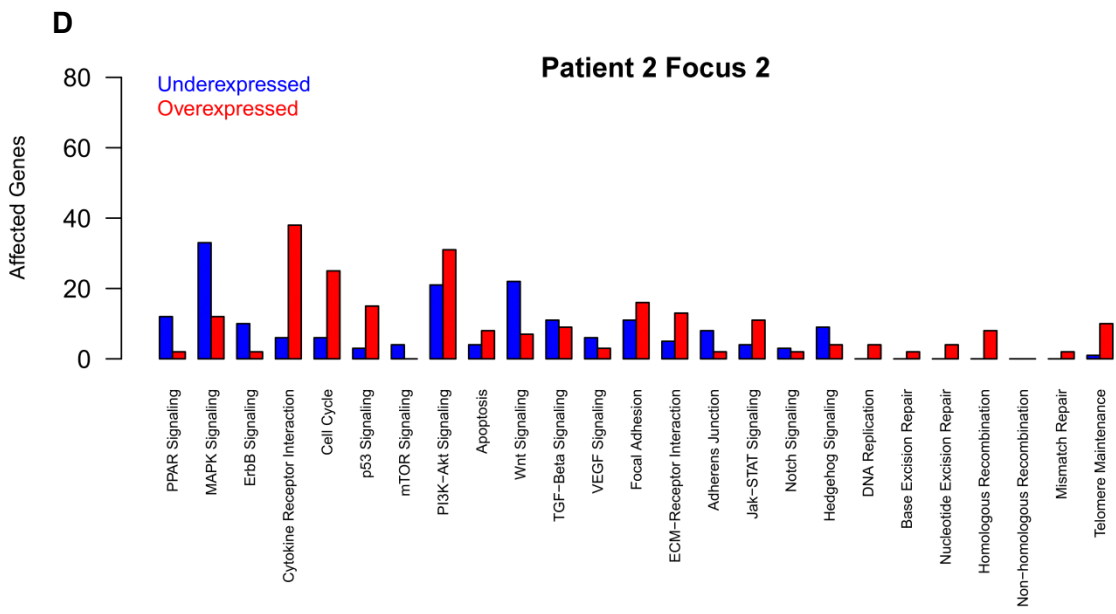
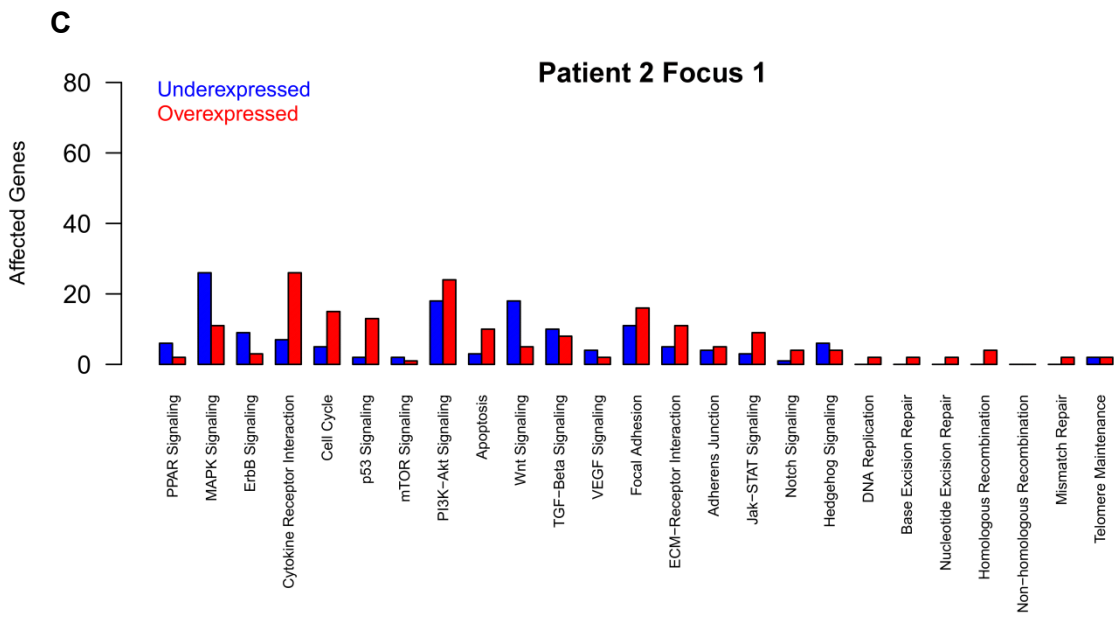


Figure S3: Different breakpoints of *EGFR* and *CDKN2A/B* CNVs in 6 patients with multifocal GBM as detected by array-CGH **Above:** High-level amplification of *EGFR* (cytoband 7p11.2) was observed in all patients (10/12 foci). The start and end positions of the breakpoints involved in the amplification were dissimilar between tumor foci of the same patients in most cases (indicated by blue and red lines) and identical in only one case (patient 4, green lines). **Below:** Homozygous deletions of the region containing *CDKN2A/B* (cytoband 9p21.3) are found in all patients but not all foci. The start and end positions of the breakpoints are indicated by blue and red lines in the case of dissimilar breakpoints and by green lines when the breakpoints were identical between tumor foci of the same patient.

Pathway enrichment of differentially regulated genes in six glioblastoma foci from four patients





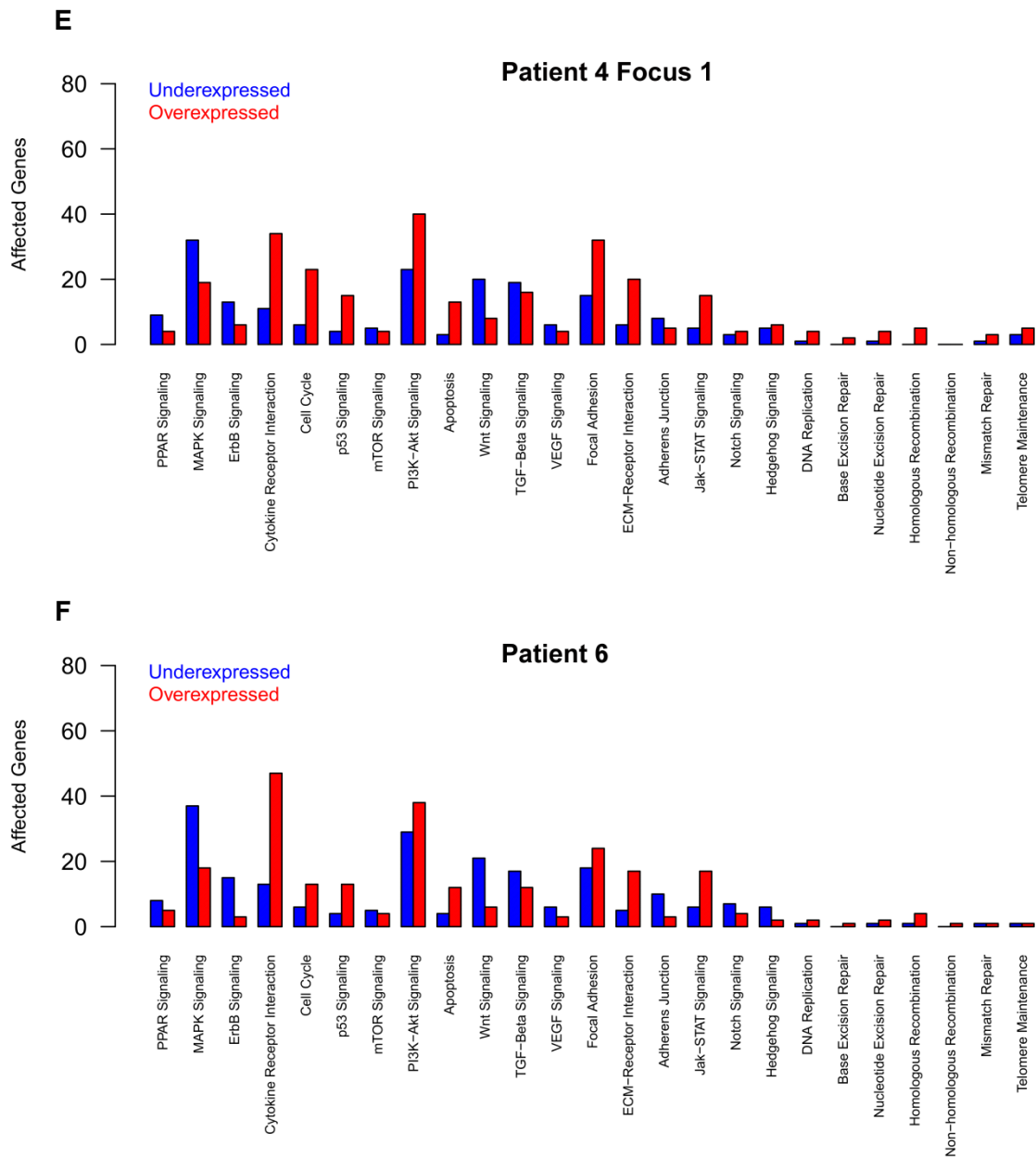


Figure S4 A-F: pathway enrichment of differentially regulated genes in six GBM foci from four patients against three commercially obtained normal brain reference RNAs. Differentially regulated genes from microarray analysis of six GBM foci from four patients with multifocal GBM were determined using an autoregressive Hidden Markov Model with second-order state-transitions as described in Seifert *et al.* [3]. Pathway enrichment was done on Kyoto Encyclopedia of Genes and Genomes (KEGG) cancer pathways and additional cancer-relevant pathways such as those involved in DNA repair, telomere maintenance, DNA replication and the Hedgehog signaling pathway. Each tumor is represented by one bar graph. The pathways are mapped to the X-axis while the number of genes is on the Y-axis. Each bar represents the number of genes in each pathway with the red bars denoting overexpressed genes and the blue bars underexpressed genes.

References:

- [1] Krex D, Mohr B, Appelt H, Schackert HK, Schackert G (2003) Genetic analysis of a multifocal glioblastoma multiforme: a suitable tool to gain new aspects in glioma development. *Neurosurgery* 53(6):1377-1384
- [2] Yoshimoto K, Dang J, Zhu S, Nathanson D, Huang T, Dumont R, Seligson DB, Yong WH, Xiong Z, Rao N, Winther H, Chakravarti A, Bigner DD, Mellinghoff IK, Horvath S, Cavenee WK, Cloughesy TF, Mischel PS (2008) Development of a Real-time RT-PCR Assay for Detecting EGFRvIII in Glioblastoma Samples. *Clin Cancer Res* 14(2):488-493. Doi:10.1158/1078-0432.CCR-07-1966
- [3] Seifert M, Abou-El-Ardat K, Friedrich B, Klink B, Deutsch A (2014) Autoregressive higher-order hidden markov models: exploiting local chromosomal dependencies in the analysis of tumor expression profiles. *PLoS One* 9(6):e100295. doi:10.1371/journal.pone.0100295